Metal-insulator transition in the disordered Hubbard model of the Lieb lattice

Yueqi Li,[1,*] Lingyu Tian [1,*] Tianxing Ma [1,2,†] and Hai-Qing Lin[3,2,1]

[1]*Department of Physics, Beijing Normal University, Beijing 100875, China*
[2]*Beijing Computational Science Research Center, Beijing 100193, China*
[3]*School of Physics, Zhejiang University, Hangzhou 310058, China*

Using the determinant quantum Monte Carlo method, we investigate the metal-insulator transition in the interacting disordered Hubbard model of a Lieb lattice in which the system characterizes the flat band centered at the Fermi level. By choosing suitable electron densities, we ensure the weak interaction sign problem to improve the reliability of our results. It is found that disorder and on-site Coulomb repulsive interaction produce interesting effects that induce the metal-insulator transition which is impossible in the half-filled case. The density of states at the Fermi energy is still finite in the thermodynamic limit, suggesting that the system is an Anderson insulator rather than a Mott insulator. Moreover, this doping system is paramagnetic, unlike the half-filled system which is ferrimagnetic.

I. INTRODUCTION

A series of experiments demonstrated the appearance of a conducting phase in a Si/SiGe heterostructure [1–3] and silicon metal-oxide-semiconductor field-effect transistors [4–6] as the electron density is varied. These findings contradict the standard scaling theory of localization, which claims that a metal-insulator transition (MIT) cannot exist in a two-dimensional (2D) noninteracting system with disorder [7,8]. In a low-density system, since the ratio of Coulomb repulsion to kinetic energy is large, the electron-electron interaction is important in the disordered system, which has also been discussed in Refs. [9,10] and is likely responsible for the metallic behavior.

In most realistic systems, both repulsion and disorder have comparable magnitudes [11] and the interplay between them has been widely studied and gives rise to several unusual phenomena [12–15]. Finkel'stei first discussed this interplay under magnetic filed and magnetic impurities [16] and Gulácsi deduced exact multielectronic ground states of disordered interacting system at and below quarter filling [17]. There are also many studies on transport and magnetic properties. For example, using quantum Monte Carlo (QMC) approaches to the Anderson-Hubbard model of a square lattice, repulsive interaction significantly enhances the DC conductivity and then induces a metal-insulator transition at quarter filling [18]. On the honeycomb lattice, the study found that disorder suppresses long-range antiferromagnetic order and induces a novel nonmagnetic insulating phase [19]. All of these phenomena illustrate the necessity of considering electronic correlation in disordered systems.

The flat-band system, which ranges from optical lattices [20–22] to ultracold atomic gases [23,24] to photonic devices [25–28], is another issue in modern condensed matter physics. Although it has been theoretically understood for three decades, this system continues to receive a great deal of attention, in particular, with regards to its ability to realize new many-body phases [29–32]. Twisted bilayer graphene is a striking example of this [33,34]. One of the simplest flat-band 2D systems is the Lieb lattice, which is also known as the side-centered square lattice. There are three types of sites, labeled A, B, and C, in each unit cell outlined by the dotted square in Fig. 1(a). For the infinite lattice with only nearest-neighbor hopping, the Lieb lattice is a three-band structure that consists of two dispersion bands $\epsilon_{\pm}(\mathbf{k}) = \pm t\sqrt{4 + 2\cos(\mathbf{k} \cdot \mathbf{a}_1) + 2\cos(\mathbf{k} \cdot \mathbf{a}_2)}$ and one dispersionless, macroscopically degenerate flat band $\epsilon(\mathbf{FB}) = 0$ centered at the Fermi level. These three bands touch each other at the M point (π, π), where the low-energy spectrum behaves as a single Dirac cone in the Brillouin zone, as shown in Fig. 1(b).

Recently, the electronic Lieb lattice was realized in surface state electrons using CO molecules and Cu(111), providing a realistic system to explore physical properties [35,36]. Furthermore, in the experiment, the atoms can also be arranged into the Lieb lattice, similar to the CuO_2 plane of cuprate superconductors [37–40].

The Hubbard model is the simplest model to use in investigation of the interaction between particles. At half filling, studies of the flat-band Lieb lattice revealed interesting physics: the system behaves as a topologically trivial gapless insulator when the Coulomb repulsion $U = 0$, but it behaves as a Mott insulator when $U > 0$ [41], and the topological phase transition caused by the spin-orbit coupling is connected to the presence of a nondispersive flat band [42]. The Lieb theorem states that bipartite lattices with two sublattices that have different sites, $N_A \neq N_B$, have a ferromagnetic state at half filling with on-site Coulomb repulsion

---

*These authors contributed equally to this work.
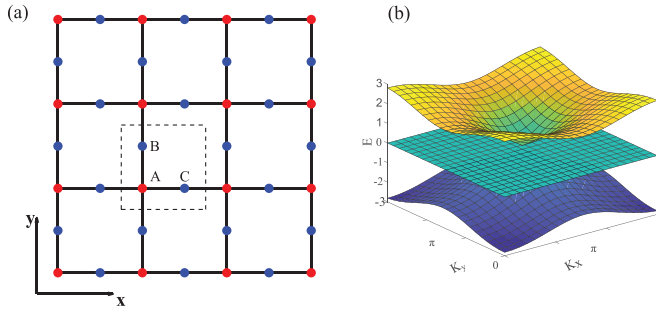†txma@bnu.edu.cn

FIG. 1. (a) Structure of the Lieb lattice. The dotted square shows one unit cell containing three lattice sites with indices A, B, and C. (b) The band structure of the tight-binding model of the Lieb lattice.

only when electron hopping between different sublattices is considered [43]. The QMC simulations showed that the local moment is strongly dependent on B/C sites due to the decreased itinerancy caused by fewer neighbors, and a metal without any magnetic ordering is found only if the repulsive effect is considered at A sites [44]. In addition, when the interaction strength at sites is switched off randomly, an insulator-to-metal transition and magnetic transition will occur simultaneously [45]. However, because of the infamous sign problem, most studies focused on half filling, and research on doping is highly important.

In this paper, our simulations are completed by the exact determinant quantum Monte Carlo (DQMC) method for cases with different fillings. For systems with varying on-site Coulomb repulsion U, disorder Δ, and electron density $\langle n \rangle$, the DC conductivity is calculated to distinguish between metallic and insulating phases. For conditions far from half filling, we focus on $\langle n \rangle = 0.3$ and 0.5, for which the sign problem is less significant compared to cases with other densities and we reveal the appearance of U- and Δ-inducing metal-insulator transitions that are absent in the half-filled case. We find that repulsion plays a delocalized role on electrons, whereas disorder plays the opposite role. In the thermodynamic limit, the finite density of states at Fermi energy suggests that the insulator is an Anderson insulator instead of a Mott insulator. Our results extend the understanding of the metal-insulator transition and magnetic order in the Lieb lattice.

II. MODEL AND METHOD

Our model is characterized by an interacting disordered Hubbard model of a Lieb lattice. The Hamiltonian, using periodic boundary conditions, reads

$$H = H_0 + H_\mu + H_U,$$

$$H_0 = -\sum_{\alpha\alpha'\langle \mathbf{i},\mathbf{j}\rangle\sigma} t_{\mathbf{ij}}(\hat{c}^\dagger_{\alpha\mathbf{i}\sigma}\hat{c}_{\alpha'\mathbf{j}\sigma} + \text{H.c.}),$$

$$H_\mu = -\mu \sum_{\alpha\mathbf{i}\sigma} \hat{c}^\dagger_{\alpha\mathbf{i}\sigma}\hat{c}_{\alpha\mathbf{i}\sigma},$$

$$H_U = U \sum_{\alpha\mathbf{i}} \left(\hat{n}_{\alpha\mathbf{i}\uparrow} - \frac{1}{2}\right)\left(\hat{n}_{\alpha\mathbf{i}\downarrow} - \frac{1}{2}\right), \quad (1)$$

where $\langle \mathbf{i}, \mathbf{j} \rangle$ runs over all pairs of nearest-neighbor sites on the lattice and $\hat{c}^\dagger_{\alpha\mathbf{i}\sigma}$ ($\hat{c}_{\alpha\mathbf{i}\sigma}$) is the creation (annihilation) operator for fermion on site $\mathbf{i}$ of the $\alpha(\alpha')$ sublattice ($\alpha/\alpha' = A, B, C$), satisfying anticommutation relations $\{\hat{c}^\dagger_{\alpha\mathbf{i}}, \hat{c}_{\alpha\mathbf{j}}\} = \delta_{\mathbf{ij}}$ and $\{\hat{c}_{\alpha\mathbf{i}}, \hat{c}_{\alpha\mathbf{j}}\} = 0$, and H.c. stands for the Hermitian conjugate. Disorder is introduced by taking the hopping parameters $t_{\mathbf{ij}}$ from a probability distribution, $P(t_{\mathbf{ij}}) = 1/\Delta$, for $t_{\mathbf{ij}} \in [t - \Delta/2, t + \Delta/2]$ and zero otherwise. Δ is a measure of the strength of the disorder and t the unit of energy is set to 1 throughout our paper. The on-site Coulomb repulsive interaction is parameterized by U and the electronic densities of system $\langle n \rangle$, denoted as the average number of electrons per site, are controlled by chemical potential μ. When $\mu = 0$, our method ensures that the system becomes half-filled and remains particle-hole symmetric without the sign problem, even with the existence of bonding disorder. $\hat{n}_{\alpha\mathbf{i}\sigma} = \hat{c}^\dagger_{\alpha\mathbf{i}\sigma}\hat{c}_{\alpha\mathbf{i}\sigma}$ is the number operator on site $\mathbf{i}$ of the α sublattice.

We employ the DQMC approach to study the Lieb lattice for on-site Coulomb repulsion. In this method, the partition function Z is expressed as $Z = Tre^{-\beta H}$ and is then approximated by a path integral using Trotter-Suzuki decomposition [46,47], which divides the imaginary-time interval $[0, \beta]$ into M equal subintervals of width $\Delta\tau = \beta/M$. The interaction term formed in the term of quartic fermion operators is decoupled through a Hubbard-Stratonovich (HS) transformation [48], and thus introduces the fluctuating fields by Ising variables. The resulting Hamiltonian quadratic form can be integrated analytically and represented as the product of the determinant of spin-up and spin-down determinants. The physical quantity proceeds with Monte Carlo sampling, which stochastically changes the space- and imaginary time-dependent auxiliary field $\mathcal{X}$. One the DQMC sweep is composed of traversing the entire site, and in our simulation, we used 8000 warmup sweeps to arrive at equilibrium state and 24 000–150 000 measuring sweeps to compute. There are two sources of statistical error in our results: one is induced by the Trotter error $\Delta\tau$, we set $\Delta\tau = 0.1$, which confirms that the error generated is small enough to neglect [49]; the other is due to disorder averaging, and we reduce this error by averaging the results from 20 disorder realizations. The authors of Ref. [50] proved that the computed data are already consistent for realization numbers larger than 10.

Under DQMC method, we can obtain the average fermion sign $\langle \text{sign} \rangle$ by computing the ratio of the integral of the product of up and down spin determinants, to the integral of the absolute value of the product [51]

$$\langle \text{sign} \rangle = \frac{\sum_{\mathcal{X}} \det M_\uparrow(\mathcal{X}) \det M_\downarrow(\mathcal{X})}{\sum_{\mathcal{X}} |\det M_\uparrow(\mathcal{X}) \det M_\downarrow(\mathcal{X})|}, \quad (2)$$

here, $M_\sigma(\mathcal{X})$ represents each spin specie matrix.

With the aim of investigating the metal-insulator transition, we computed the T-dependent DC conductivity, which can be obtained using the wave vector $\mathbf{q}$ and the imaginary (Matsubara) time τ-dependent current-current correlation function Λ_{xx},

$$\sigma_{dc}(T) = \frac{\beta^2}{\pi}\Lambda_{xx}\left(\mathbf{q} = 0, \tau = \frac{\beta}{2}\right), \quad (3)$$

where $\Lambda_{xx}(\mathbf{q}, \tau) = <\hat{j}_x(\mathbf{q}, \tau)\hat{j}_x(-\mathbf{q}, 0)>$, β is the reciprocal of temperature and $\hat{j}_x(\mathbf{q}, \tau)$ is the Fourier transform of the

current density operator $\hat{j}_x(\mathbf{i}, \tau)$ in the x direction. This formula is valid only if the temperature is lower than the energy scale. Thus, the high-order term of the Taylor expansion formula of the frequency-dependent function of conductance needs to be sufficiently small [52]. In the disordered system that we study, the energy scale is set by the disorder strength Δ so that Eq. (3) is valid at low temperatures, and we judge the phase transition mainly by the result $T \lesssim 0.25$. The temperatures are much smaller than disorder strength, and all results are valid for the studied disorder strength. It is worth mentioning that the equation was used in the disordered Hubbard model [18,19,53,54], whereas it is still applied to a system without disorder [19,55]. A further way to distinguish the type of insulating phase is the density of states (DOS) at Fermi energy [53,56]

$$N(0) \simeq \beta \times G(\mathbf{r} = 0, \tau = \beta/2), \tag{4}$$

where G is the imaginary time Green's function. We are interested in the magnetic behavior of the system by focusing on the space equal-time spin-spin correlation function [57], defined as

$$C(r) = < S^z(\mathbf{R}_i + \mathbf{r}) S^z(\mathbf{R}_i) >, \tag{5}$$

where $S^z(\mathbf{R}_i) = n_{i\uparrow} - n_{i\downarrow}$. From $C(\mathbf{r})$, we can obtain the spin structure factor $S(\mathbf{q})$ through the Fourier transform

$$S(\mathbf{q}) = \sum_{\mathbf{r}} e^{i\mathbf{q}\cdot\mathbf{r}} C(\mathbf{r}). \tag{6}$$

Then, we define the $\mathbf{q}$-dependent susceptibility as $\chi(\mathbf{q}) = \beta S(\mathbf{q})$ [18]. The wave vectors $\mathbf{q} = (0, 0)$ yield the ferromagnetic (FM) susceptibility, and $\mathbf{q} = (\pi, \pi)$ yields the antiferromagnetic (AF) susceptibility [58]. For the Lieb lattice with ideal antiferromagnetic distribution, the spin direction of same sublattices (AA, BB, CC) and next-nearest neighbor sublattices (BC) is the same, and the spin direction of the nearest-neighbor sublattices is opposite, so the AF structure factor in our paper is calculated by the formula $S_{AF} = S_{AA}^z + S_{BB}^z + S_{CC}^z - S_{AB}^z - S_{AC}^z - S_{BA}^z - S_{CA}^z + S_{BC}^z + S_{CB}^z$, where each term that contributes to AF is considered, and the form of the equation is unaffected no matter how the electrons are distributed on the $A/B/C$ sites [59].

III. RESULT AND DISCUSSION

First, we plot the DC conductivity as a function of temperature under a few representative U and Δ at half filling. The total number of lattice sites we focus on in this paper is $N = 3 \times L^2$ with $L = 8$ unless otherwise specified. Figure 2(a) shows that keeping the disorder strength $\Delta = 1.0$, the DC conductivity decreases with increasing repulsive interaction strength. In the case of higher temperatures, σ_{dc} increases as the temperature decreases, while in the case of $T \leqslant 0.2$, σ_{dc} starts to decrease, indicating insulating behavior. The effect of disorder on the DC conductivity with the intermediate repulsive interaction $U = 4.0$ is shown in Fig. 2(b), where increasing the hopping disorder strength reduces the value of the DC conductivity. Neither increases in the hopping disorder strength nor the interaction strength can change the insulating state at half filling. Our finding that there is no metal-insulator
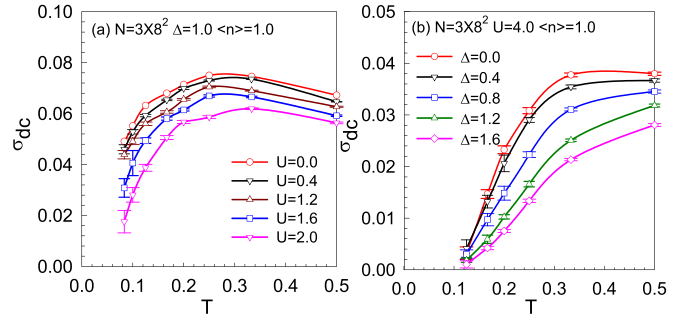

FIG. 2. Temperature dependence of the DC conductivity σ_{dc} computed on the $N = 3 \times 8 \times 8$ lattice for (a) various interaction strengths at $\Delta = 1.0$ and (b) various disorder strengths at $U = 4.0$. Data points are averages over 20 disorder realizations.

transition in the hopping-disordered Hubbard model at half filling is consistent with previous results [44].

Our simulation is aimed at understanding the physical properties when the band is far from half filling. The fermion sign problem is protected by the particle-hole symmetry at exactly half filling, while our simulations are plagued by the sign problem when doping away from half filling [60] and this restricts accessible temperatures. To avoid the error caused by the sign problem, we compute the relation between the sign problem and density for different temperatures and disorder strengths at fixed $U = 4.0$ in Fig. 3 with the Monte Carlo parameters of 24 000 times runs. As $\langle n \rangle$ decreases from 1, $\langle \text{sign} \rangle$ decreases rapidly to 0 and floats about 0 until $\langle n \rangle = 0.7$. Then, as $\langle n \rangle$ gradually decreases to 0, $\langle \text{sign} \rangle$ recovers to 1. $\langle \text{sign} \rangle$ shows no signal as it passes through $\langle n \rangle = 2/3$, which corresponds to entry into the flat band. Figure 3(a) shows the inverse temperature β dependence of the sign; increasing β leads to a more severe sign problem. Indeed, the average sign decays exponentially with increasing β [51]. Conversely, increasing the disorder strength ameliorates the sign problem, as shown in Fig. 3(b). Avoiding densities with a more serious sign problem such as $\langle n \rangle = 0.4$, we choose two densities of $\langle n \rangle = 0.3$ and $\langle n \rangle = 0.5$ to study the effect of doping on the transport and magnetic properties. For the results where the sign problem is not too serious, longer runs can help compensating the fluctuations. In fact, the runs can be estimated to be stretched by a factor on the order of $\langle \text{sign} \rangle^{-2}$ [61,62]. In our
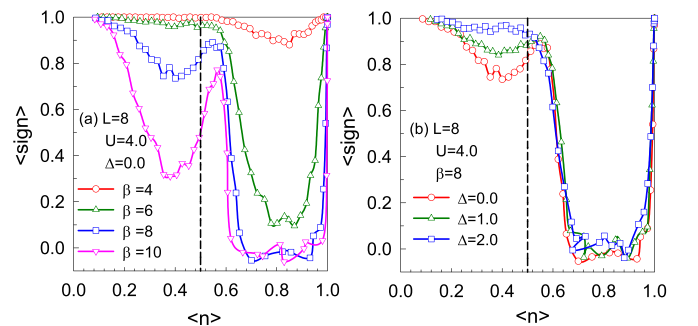

FIG. 3. Sign problem $\langle \text{sign} \rangle$ as a function of density for (a) different temperatures and (b) various disorder strengths. The dashed line represents $\langle n \rangle = 0.5$.
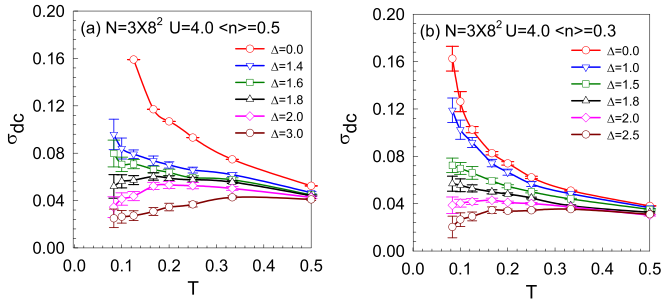
FIG. 4. The DC conductivity as a function of temperature for various disorder strengths at $\langle n \rangle = 0.5$ and $\langle n \rangle = 0.3$.

FIG. 6. The DC conductivity as a function of temperature for various interaction strengths at $\langle n \rangle = 0.5$ and $\langle n \rangle = 0.3$.

simulations, some of the results are computed with 150 000 runs to obtain the same quality of data as $\langle \text{sign} \rangle \sim 1.0$.

In Fig. 4(a), we show the behavior of the DC conductivity for a range of disorder strengths at $\langle n \rangle = 0.5$ and $U = 4.0$. The DC conductivity curve below $\Delta = 1.6$ is concave ($d\sigma_{dc}/dT < 0$) at low T, indicating a metallic phase, while above $\Delta = 1.8$, the curve is convex ($d\sigma_{dc}/dT > 0$), corresponding to an insulating phase. This figure displays a transition from metallic to insulating behavior at a critical disorder strength of $\Delta_c = 1.6$–1.8, completely differing from the half filling case [see Fig. 2(a)]. Similarly, $\Delta_c = 1.8 \sim 2.0$ at $\langle n \rangle = 0.3$ for $U = 4.0$. This indicates that disorder localizes the electrons. We also focus on the effect of doping on transport properties. For example, when keeping other parameters constant ($\Delta = 1.4$ and $U = 4.0$), the system at $\langle n \rangle = 0.3, 0.5$ is metallic, but is insulating at half filling; see Fig. 2(b), suggesting that doping can lead to the metal-insulator transition.

The difference between the square lattice and Lieb lattice lies at the flat band; thus, one can compare the physical properties of these two lattices to analyze the importance of the flat band. To verify the flat band in a disordered system, we compute the total energy as a function of density in the noninteracting limit. In Fig. 5, the addition of disorder changes the energy level and destroys its degeneracy when $\langle n \rangle < 2/3$ and $\langle n \rangle > 4/3$. However, the band structure is hardly influenced by disorder when $\langle n \rangle \in (2/3, 4/3)$, the range of filling density which corresponds to the flat band, suggesting that disorder has little effect on the flat band. Thus we can refer to the results of the disordered system in our paper to discuss the role of the flat band. At half filling, the Lieb lattice exhibits weaker

metallicity than the square lattice with the same parameters; see Fig. 2(b) and Fig. 1 in Ref. [18]. A similar phenomenon also appears at $\langle n \rangle = 0.3, 0.5$ when the flat band is empty. Thus, the flat band will suppress transport properties regardless of whether the electrons have filled the flat band.

To observe the role of the interaction U on the DC conductivity, we compare the σ_{dc} behavior of different interactions. The value of disorder strength we choose is 1.5, so that the system size is larger than the localization length and the disordered noninteracting system is insulating. Figure 6 displays the temperature dependence of the DC conductivity for electronic density $\langle n \rangle = 0.5$ and 0.3. The interaction is found to play a profound role in the DC conductivity: in the high-temperature regime, the interaction slightly reduces σ_{dc}. In contrast, in the low-temperature regime, upon turning on the interaction, the value of σ_{dc} starts to increase, and a noninteracting insulating phase gradually changes into a metallic phase at approximately $U = 1.0$. This phenomenon indicates that the interaction has a delocalizing effect on the electrons in the disordered systems. The single-particle gap is another electronic property we are interested in. At half filing, the Hubbard model of the the Lieb lattice shows a charge excitation gap for $U > 0$ without disorder, i.e., the properties of a Mott insulator. Since the Anderson insulator is gapless at the Fermi level, the gap can be used to determine the type of the insulating phase although the gap is unaffected by the order parameter of symmetry breaking. Here, we use the density of states at the Fermi energy to extract the single-particle gap. In Fig. 7 DOS is plotted as a function of temperature
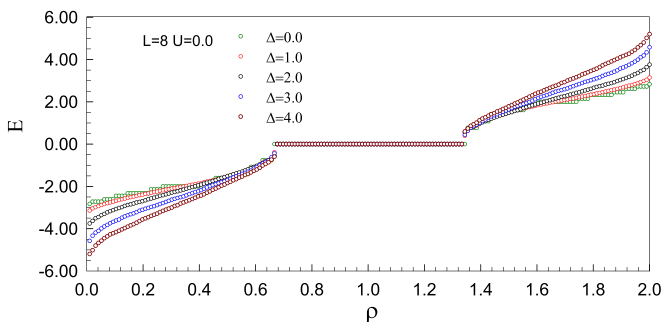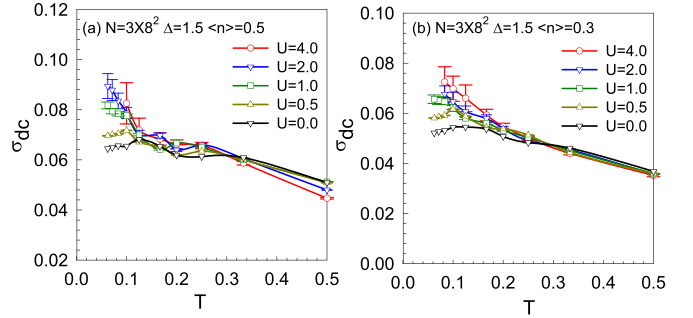

FIG. 5. Total energy as a function of electronic density for the $L = 8$ lattice in the noninteracting limit. $\langle n \rangle \in (2/3, 4/3)$ corresponds to the flat-band filling.
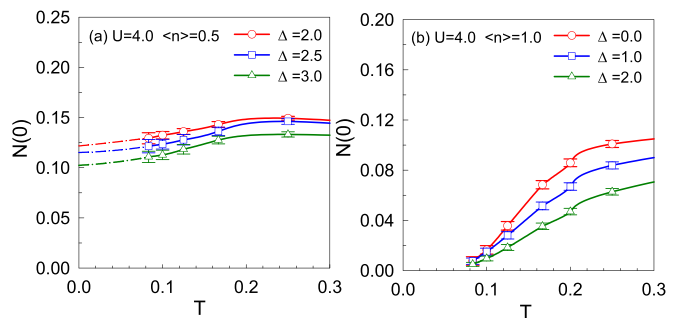

FIG. 7. The density of states as a function of temperature at (a) $\langle n \rangle = 0.5$ and (b) $\langle n \rangle = 1.0$ for $U = 4.0$ for various disorder strengths.
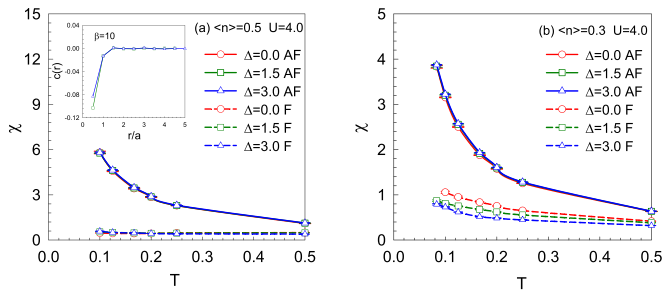
FIG. 8. (a) The ferromagnetic and antiferromagnetic susceptibility as a function of temperature at $\langle n \rangle = 0.5, 0.3$ for $U = 4.0$. Inset: Spatial dependence of the spin-spin correlation function at $\beta = 10$. r running along a horizontal line, i.e., line with alternating red and blue sites in Fig. 1(a).

FIG. 9. The conductivity as a function of temperature (a) with different lattice sizes $L = 8$, 12, (b) with various disorder strengths for $L = 12$ and $\langle n \rangle = 0.5$.

for various disorder strengths and fixed on-site Coulomb repulsive interaction at different densities. One can see that $N(0)$ decreases with decreasing temperature for all cases. When $T \to 0$, DOS will converge to finite values at $\langle n \rangle = 0.5$, suggesting the presence of the Anderson insulator. With increasing intensity of disorder, the value of DOS decreases in the thermodynamic limit but is finite. The finite density of states forms an interesting counterpoint to that of the Mott insulator whose DOS converges to zero, as shown in Fig. 7(b). Finally, we consider the effect of doping on magnetic order. Figure 8 provides the dependence of susceptibility χ on T for $U = 4.0$ and various disorder strengths. In all cases, it can be seen that the ferromagnetic susceptibility χ_{FM} increases slightly with decreasing temperature, while the antiferromagnetic susceptibility χ_{AF} increases significantly and is always stronger than χ_{FM}. Although χ_{AF} increases rapidly when T approaches 0, it is still not enough to prove that there is an antiferromagnetic order in our system. If there was perfect order, χ_{AF} should approach $\beta * N$ when $T \to 0$; however, χ_{AF} here is much smaller than this value. In the inset of Fig. 8(a), inhibition of disorder is only apparent in non-nearest-neighbor terms, which contribute little to antiferromagnetism; perhaps this is why disorder has little effect on magnetic susceptibility. Overall, Fig. 8 proves that the doped system is paramagnetic, while the half-filled system is ferromagnetic [44], indicating doping can change the magnetic properties.

IV. CONCLUSION

In summary, we studied a doped Lieb lattice containing both on-site Coulomb repulsion and disorder using a determinant quantum Monte Carlo method. We computed the half-filled case to examine our method and explored the sign problem at states far away from half filling. The sign problem becomes more serious with decreasing temperature
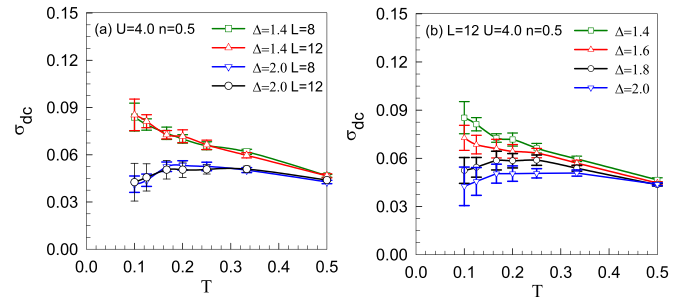
and weaker with increasing disorder strength. To ensure the reliability of the results, we chose two electron densities where the sign problem is less severe. We calculate the temperature-dependent DC conductivity σ_{dc} and found that Hopping disorder drives the metallic phase to the insulating phase, while Coulomb repulsion has the opposite effect. Compared to the previous theoretical results on the half-filled case, the produced insulating phase is proven to be an Anderson insulator by studying the density of states in the Fermi energy. In addition, data on the susceptibility $\chi(T)$ suggested that the doping system is in a paramagnetic state. Compared to the ferrimagnetic half-filled system, it can be inferred that doping can change lattice magnetic properties.

APPENDIX: FINITE-SIZE EFFECT

To ascertain that the insulating phase produced by disorder at low T is not due to the system size being smaller than the localization length, we study the conductivity response for varying system size. We find that the size affects weakly on conductivity regardless of whether the system is in an insulating or metallic phase, as shown in Fig. 9(a). We also focus on the relationship between σ_{dc} and T at different disorder for $L = 12$ and $\langle n \rangle = 0.5$. In Fig. 9(b), the behavior of conductivity at $L = 12$ is almost the same as the one at $L = 8$, and the critical disorder-inducing phase transition is also around 1.6–1.8. These results demonstrate the reliability of our conclusion that disorder induces the metal-insulator transition when doping away from half filling.

[1] J. Lam, M. D'Iorio, D. Brown, and H. Lafontaine, Phys. Rev. B **56**, R12741 (1997).

[2] A. Shashkin and S. Kravchenko, Ann. Phys. (NY) **435**, 168542 (2021).

[3] A. A. Shashkin and S. V. Kravchenko, Applied Sciences **9**, 1169 (2019).

[4] S. V. Kravchenko, W. E. Mason, G. E. Bowker, J. E. Furneaux, V. M. Pudalov, and M. D'Iorio, Phys. Rev. B **51**, 7038 (1995).

[5] S. V. Kravchenko, D. Simonian, M. P. Sarachik, W. Mason, and J. E. Furneaux, Phys. Rev. Lett. **77**, 4938 (1996).

[6] E. Abrahams, S. V. Kravchenko, and M. P. Sarachik, Rev. Mod. Phys. **73**, 251 (2001).

[7] E. Abrahams, P. W. Anderson, D. C. Licciardello, and T. V. Ramakrishnan, Phys. Rev. Lett. **42**, 673 (1979).

[8] B. Hetényi, S. Parlak, and M. Yahyavi, Phys. Rev. B **104**, 214207 (2021).

[9] M. Y. Melnikov, A. A. Shashkin, V. T. Dolgopolov, A. Y. X. Zhu, S. V. Kravchenko, S.-H. Huang, and C. W. Liu, Phys. Rev. B **99**, 081106(R) (2019).

[10] A. A. Shashkin, M. Y. Melnikov, V. T. Dolgopolov, M. M. Radonjić, V. Dobrosavljević, S.-H. Huang, C. W. Liu, A. Y. X. Zhu, and S. V. Kravchenko, Phys. Rev. B **102**, 081119(R) (2020).

[11] V. Dobrosavljevic, arXiv:1112.6166.

[12] Y. Otsuka, Y. Morita, and Y. Hatsugai, Phys. Rev. B **58**, 15314 (1998).

[13] R. Berkovits and J. W. Kantelhardt, Phys. Rev. B **65**, 125308 (2002).

[14] M. E. Pezzoli and F. Becca, Phys. Rev. B **81**, 075106 (2010).

[15] P. A. Lee and T. V. Ramakrishnan, Rev. Mod. Phys. **57**, 287 (1985).

[16] A. M. Finkel'shtein, Sov. Phys. JETP **59**, 212 (1984).

[17] Z. Gulácsi, Phys. Rev. B **69**, 054204 (2004).

[18] P. J. H. Denteneer, R. T. Scalettar, and N. Trivedi, Phys. Rev. Lett. **83**, 4610 (1999).

[19] T. Ma, L. Zhang, C.-C. Chang, H.-H. Hung, and R. T. Scalettar, Phys. Rev. Lett. **120**, 116601 (2018).

[20] S. Taie, H. Ozawa, T. Ichinose, T. Nishio, S. Nakajima, and Y. Takahashi, Sci. Adv. **1**, e1500854 (2015).

[21] H. Ozawa, S. Taie, T. Ichinose, and Y. Takahashi, Phys. Rev. Lett. **118**, 175301 (2017).

[22] R. Shen, L. B. Shao, B. Wang, and D. Y. Xing, Phys. Rev. B **81**, 041410(R) (2010).

[23] R. A. Hart, P. M. Duarte, T.-L. Yang, X. Liu, T. Paiva, E. Khatami, R. T. Scalettar, N. Trivedi, D. A. Huse, and R. G. Hulet, Nature (London) **519**, 211 (2015).

[24] F. A. An, E. J. Meier, and B. Gadway, Phys. Rev. X **8**, 031045 (2018).

[25] Y. Zong, S. Xia, L. Tang, D. Song, Y. Hu, Y. Pei, J. Su, Y. Li, and Z. Chen, Opt. Express **24**, 8877 (2016).

[26] Y. Nakata, T. Okada, T. Nakanishi, and M. Kitano, Phys. Rev. B **85**, 205128 (2012).

[27] R. A. Vicencio, C. Cantillano, L. Morales-Inostroza, B. Real, C. Mejía-Cortés, S. Weimann, A. Szameit, and M. I. Molina, Phys. Rev. Lett. **114**, 245503 (2015).

[28] S. Mukherjee, A. Spracklen, D. Choudhury, N. Goldman, P. Öhberg, E. Andersson, and R. R. Thomson, Phys. Rev. Lett. **114**, 245504 (2015).

[29] A. Julku, S. Peotta, T. I. Vanhala, D.-H. Kim, and P. Törmä, Phys. Rev. Lett. **117**, 045303 (2016).

[30] L. Liang, T. I. Vanhala, S. Peotta, T. Siro, A. Harju, and P. Törmä, Phys. Rev. B **95**, 024515 (2017).

[31] S. Peotta and P. Törmä, Nat. Commun. **6**, 8944 (2015).

[32] M. Maksymenko, A. Honecker, R. Moessner, J. Richter, and O. Derzhko, Phys. Rev. Lett. **109**, 096404 (2012).

[33] Y. Cao, V. Fatemi, A. Demir, S. Fang, S. L. Tomarken, J. Y. Luo, J. D. Sanchez-Yamagishi, K. Watanabe, T. Taniguchi, E. Kaxiras, R. C. Ashoori, and P. Jarillo-Herrero, Nature (London) **556**, 80 (2018).

[34] Y. Cao, V. Fatemi, S. Fang, K. Watanabe, T. Taniguchi, E. Kaxiras, and P. Jarillo-Herrero, Nature (London) **556**, 43 (2018).

[35] M. R. Slot, T. S. Gardenier, P. H. Jacobse, G. C. P. van Miert, S. N. Kempkes, S. J. M. Zevenhuizen, C. M. Smith, D. Vanmaekelbergh, and I. Swart, Nat. Phys. **13**, 672 (2017).

[36] R. Drost, T. Ojanen, A. Harju, and P. Liljeroth, Nat. Phys. **13**, 668 (2017).

[37] C. Weeks and M. Franz, Phys. Rev. B **82**, 085310 (2010).

[38] A. Mielke, J. Phys. A: Math. Gen. **24**, L73 (1991).

[39] R. T. Scalettar, D. J. Scalapino, R. L. Sugar, and S. R. White, Phys. Rev. B **44**, 770 (1991).

[40] V. J. Emery, Phys. Rev. Lett. **58**, 2794 (1987).

[41] P. Kumar, T. I. Vanhala, and P. Törmä, Phys. Rev. B **96**, 245127 (2017).

[42] S. Jana, A. Saha, and A. Mukherjee, Phys. Rev. B **100**, 045420 (2019).

[43] E. H. Lieb, Phys. Rev. Lett. **62**, 1201 (1989).

[44] N. C. Costa, T. Mendes-Santos, T. Paiva, R. R. dos Santos, and R. T. Scalettar, Phys. Rev. B **94**, 155107 (2016).

[45] L. Oliveira-Lima, N. C. Costa, J. P. de Lima, R. T. Scalettar, and R. R. dos Santos, Phys. Rev. B **101**, 165109 (2020).

[46] M. Suzuki, Prog. Theor. Phys. **56**, 1454 (1976).

[47] R. M. Fye, Phys. Rev. B **33**, 6271 (1986).

[48] J. E. Hirsch, Phys. Rev. B **31**, 4403 (1985).

[49] R. Mondaini, K. Bouadim, T. Paiva, and R. R. dos Santos, Phys. Rev. B **85**, 125127 (2012).

[50] J. Meng, R. Mondaini, T. Ma, and H.-Q. Lin, Phys. Rev. B **104**, 045138 (2021).

[51] V. I. Iglovikov, E. Khatami, and R. T. Scalettar, Phys. Rev. B **92**, 045110 (2015).

[52] J. Wang, L. Zhang, R. Ma, Q. Chen, Y. Liang, and T. Ma, Phys. Rev. B **101**, 245161 (2020).

[53] N. Trivedi and M. Randeria, Phys. Rev. Lett. **75**, 312 (1995).

[54] N. Trivedi, R. T. Scalettar, and M. Randeria, Phys. Rev. B **54**, R3756 (1996).

[55] P. J. H. Denteneer, R. T. Scalettar, and N. Trivedi, Phys. Rev. Lett. **87**, 146401 (2001).

[56] S. Lederer, Y. Schattner, E. Berg, and S. A. Kivelson, Proc. Natl. Acad. Sci. **114**, 4905 (2017).

[57] C. N. Varney, C.-R. Lee, Z. J. Bai, S. Chiesa, M. Jarrell, and R. T. Scalettar, Phys. Rev. B **80**, 075116 (2009).

[58] P. B. Chakraborty, K. Byczuk, and D. Vollhardt, Phys. Rev. B **84**, 155123 (2011).

[59] J. Gouveia and R. Dias, J. Magn. Magn. Mater. **405**, 292 (2016).

[60] G. G. Batrouni and R. T. Scalettar, Phys. Rev. B **42**, 2282 (1990).

[61] R. dos Santos, Braz. J. Phys. **33**, 36 (2003).

[62] G. Yang, S. Xu, W. Zhang, T. Ma, and C. Wu, Phys. Rev. B **94**, 075106 (2016).